BIOCHEMISTRY
including biophysical chemistry & molecular biology
Article

Biochemistry **2010,** *49,* 5109–5116 5109
DOI: 10.1021/bi9019274

Highly Sensitive Analysis of the Interaction between HIV-1 Gag and Phosphoinositide Derivatives Based on Surface Plasmon Resonance[†]

Kensaku Anraku,[‡] Ryota Fukuda,[§] Nobutoki Takamune,[∥] Shogo Misumi,[∥] Yoshinari Okamoto,[§] Masami Otsuka,*[,§] and Mikako Fujita*[,⊥]

[‡]*Institute of Health Sciences, Kumamoto Health Science University, 325 Izumi-machi, Kumamoto 861-5598, Japan,* [§]*Department of Bioorganic Medicinal Chemistry, Faculty of Life Sciences,* [∥]*Department of Pharmaceutical Biochemistry, Faculty of Life Sciences, and* [⊥]*Research Institute for Drug Discovery, School of Pharmacy, Kumamoto University, 5-1 Oe-honmachi, Kumamoto 862-0973, Japan*

Received November 10, 2009; Revised Manuscript Received May 23, 2010

ABSTRACT: Human immunodeficiency virus type 1 (HIV-1) Gag protein is the principal structural component of the HIV particle. Localization of the $Pr55^{Gag}$ protein to the plasma membrane initiates virus assembly. Recent studies indicated that D-*myo*-phosphatidylinositol (PI) 4,5-bisphosphate (PI(4,5)P2) regulates $Pr55^{Gag}$ localization and assembly. We determined the binding affinity between $Pr55^{Gag}$ or its N-terminal MA domain and various phosphoinositide derivatives using a highly sensitive surface plasmon resonance (SPR) sensor and biotinylated inositol phosphate. The equilibrium dissociation constants obtained using this approach reflected the distinct magnitude of acyl group-based and phosphate group-based interactions. The dissociation constant (K_D) for $Pr55^{Gag}$ complexed with 1,4,5-IP3 (an inositol with divalent phosphate groups and devoid of lipid groups) was 2170 μM, while the K_D for di-C_8-PI (a lipid-containing inositol devoid of divalent phosphate groups) was 186 μM, and the K_D for di-C_8-PI(4,5)P2 (an inositol with both lipid and divalent phosphate groups) was 47.4 μM. The same trend in affinity was observed when these phosphoinositides were complexed with MA. Our results suggest that the contribution of hydrophobic acyl chains is greater than negatively charged inositol phosphates in $Pr55^{Gag}$/MA binding. Furthermore, each inositol phosphate (devoid of lipid groups) tested showed a distinct $Pr55^{Gag}$-binding affinity depending on the position and number of phosphate groups. However, the position and number of phosphate groups had no effect on MA-binding affinity.

The HIV-1[1] genome-encoded $Pr55^{Gag}$ protein is the principal structural component required for virus assembly (*1*, *2*). Following ribosomal synthesis, $Pr55^{Gag}$ is directed to the plasma membrane, where it is assembled with other components to form immature budding virions. $Pr55^{Gag}$ is composed of four major domains: matrix (MA), capsid (CA), nucleocapsid (NC), and p6, in addition to two spacer peptides: p2 and p1. The N-terminal MA domain plays a critical role in the binding of $Pr55^{Gag}$ to the plasma membrane (*3*), while the CA (*4*) and NC (*5*) domains contribute to multimerization of $Pr55^{Gag}$ and virus genome packaging, respectively. The p6 domain regulates viral budding (*6*). Concurrently or immediately following budding, $Pr55^{Gag}$ is cleaved by a viral protease to yield the mature protein of infectious HIV virions.

During membrane targeting, several thousand copies of $Pr55^{Gag}$ colocalize at lipid rafts on the plasma membrane (*7*), a process mediated by the $Pr55^{Gag}$ MA domain N-terminal myristoyl moiety and basic patch. The myristoyl group of the MA N-terminal glycine is flipped and exposed to the surface of the protein through the multimerization of $Pr55^{Gag}$, a phenomenon known as the myristoyl switch (*8*, *9*). The MA basic patch, on the other hand, binds to the acidic region of membrane phospholipids (*10*). The N-terminal myristoyl group and the conserved basic region, both of which are exposed on the surface of the MA domain, function synergistically to promote tight membrane binding. Recent studies showed that D-*myo*-phosphatidylinositol 4,5-bisphosphate (PI(4,5)P2) is the binding target of the basic patch (*11*−*13*). PI(4,5)P2, the most abundant of the PIPs, serves as the precursor of at least three second-messenger molecules: 1,4,5-IP3 (*14*), PI(3,4,5)P3 (*15*), and diacylglycerol (*16*, *17*). In addition, PI(4,5)P2 may be involved in other cellular processes, such as exocytosis, cytoskeletal regulation, and intracellular vesicle trafficking (*18*). Ono et al. identified PI(4,5)P2 as a cellular factor regulating the targeting of $Pr55^{Gag}$ to the plasma membrane (*11*). They overexpressed phosphoinositide 5-phosphatase IV, an enzyme that depletes cellular PI(4,5)P2, and found that

[†]This work was supported in part by a Grant-in-Aid for Scientific Research (B) (20390033) (to M.O.) and a Grant-in-Aid for Scientific Research (C) (19590480) (to M.F.) from the Japan Society for the Promotion of Science, by a Grant-in-Aid for Exploratory Research (19659025) (to M.O.) from the Japan Society for the Promotion of Science, and by the aid of a special fellowship (to K.A.) granted by Kumamoto Health Science University for culture, education and science.

*To whom correspondence should be addressed. Phone: +81-96-371-4620 (M.O.); +81-96-371-4622 (M.F.). Fax: +81-96-371-4620 (M.O.); +81-96-371-4624 (M.F.). E-mail: motsuka@gpo.kumamoto-u.ac.jp (M.O.); mfujita@kumamoto-u.ac.jp (M.F.).

[1]Abbreviations: HIV-1, human immunodeficiency virus type 1; SPR, surface plasmon resonance; $Pr55^{Gag}$, Gag 55-kDa precursor; MA, matrix; CA, capsid; 1,4,5-IP3, D-*myo*-inositol 1,4,5-trisphosphate; 1,3,4-IP3, D-*myo*-inositol 1,3,4-trisphosphate; 1,3,4,5-IP4, D-*myo*-inositol 1,3,4,5-tetrakisphosphate; STP, sodium tripolyphosphate; di-C_8, 1,2-di-*O*-heptanoylglyceryl; PI, D-*myo*-phosphatidylinositol; PIP, D-*myo*-phosphatidylinositol phosphate; PI(4,5)P2, D-*myo*-phosphatidylinositol 4,5-bisphosphate; PI(3,4)P2, D-*myo*-phosphatidylinositol 3,4-bisphosphate; PI(3,4,5)P3, D-*myo*-phosphatidylinositol 3,4,5-trisphosphate; PH, pleckstrin homology; PLC, phospholipase C.

Published on Web 05/24/2010

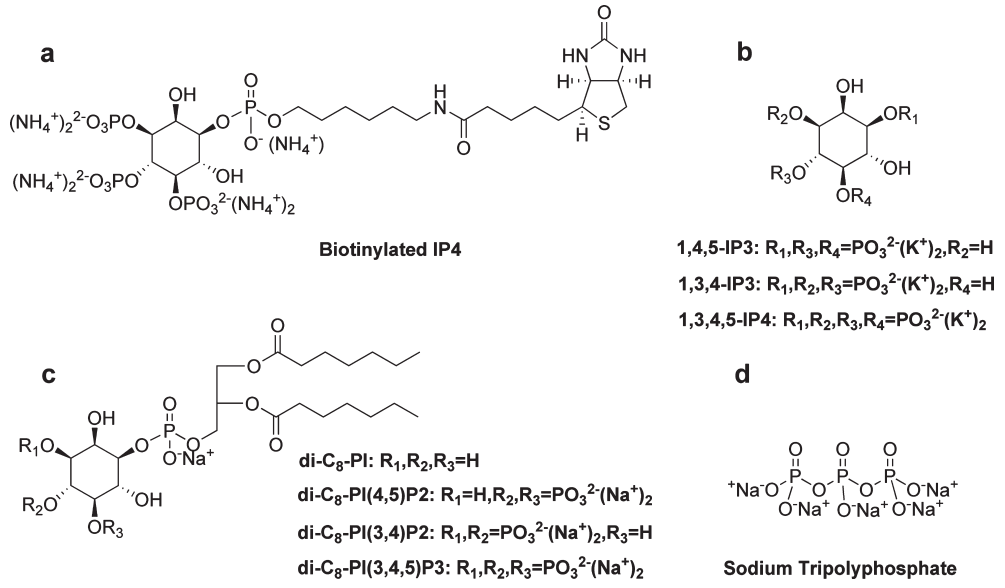

FIGURE 1: Structures of biotinylated IP4 (a), inositol phosphates (b), phosphatidylinositols (c), and sodium tripolyphosphate (d).

$Pr55^{Gag}$ no longer localized to the plasma membrane and was retargeted to late endosomes. By overexpressing ADP-ribosylation factor 6, which induces the formation of PI(4,5)P2-enriched endosomal structures, Ono et al. demonstrated that $Pr55^{Gag}$ was redirected to PI(4,5)P2-enriched vesicles (*11*). These findings were supported by mass spectrometric protein footprinting (*13*) and NMR analyses (*12*) that demonstrated direct interactions between $Pr55^{Gag}$ and PI(4,5)P2.

Using NMR, Saad et al. observed a conformational change in $Pr55^{Gag}$ induced by PI(4,5)P2-MA binding that triggers myristate exposure (*12*). They revealed an "extended lipid" conformation of the PI(4,5)P2-MA complex, in which the inositol headgroup and glycerol 2′-fatty acid chain bind to the cleft of the MA domain, and proposed a membrane binding model in which the glycerol 1′-fatty acid and exposed MA myristoyl group are inserted into the membrane. Saad et al. also determined the binding affinity between MA and phosphoinositide derivatives carrying acyl chains of variable length (chain length = 2 or 6) and found that affinity increases with acyl chain length (*12*).

Although binding of $Pr55^{Gag}$ and phosphoinositide is known to be critical for HIV-1 replication, the detailed binding mode and binding affinity of $Pr55^{Gag}$/MA−phosphoinositide complexes remain unknown. Therefore, we developed a highly sensitive *in vitro* assay to determine the binding affinity of $Pr55^{Gag}$/MA for phosphoinositide derivatives by employing a surface plasmon resonance sensor using biotinylated inositol phosphate. This enabled us to determine the equilibrium dissociation constants (K_D) of $Pr55^{Gag}$/MA and phosphoinositide complexes of biological significance.

To determine the specificity of binding of $Pr55^{Gag}$/MA for phosphoinositides, this SPR assay was conducted with phosphoinositides having a different number of phosphates and its regioisomer with or without acyl chain. For example, 1,4,5-IP3 is a second messenger that stimulates the discharge of calcium from the endoplasmic reticulum (*14*). 1,3,4,5-IP4 is a second messenger for the Ras family of GTPases (*19*). Di-C_8-PI is an artificial compound whose acyl chains are shorter than those of naturally occurring PI that forms the leaflet of the cell membrane (*20*). Di-C_8-PI(4,5)P2 is an artificial analogue of natural PI(4,5)P2, which also exists in the leaflet of the cell membrane and is the most abundant PIP (*18*), while di-C_8-PI(3,4)P2 and di-C_8-PI(3,4,5)P3 are analogues of the second messengers PI(3,4)P2 and PI(3,4,5)-P3. PI(3,4,5)P3 is particularly important as an enhancer of cell survival (*15*) and is generated when extracellular signaling induces 3-kinase activation in connection with phosphorylation of PI(4,5)P2.

EXPERIMENTAL PROCEDURES

Chemicals. Biotinylated D-*myo*-inositol-1,3,4,5-tetrakisphosphate (biotinylated IP4) (Figure 1a) was synthesized as described previously (*21*). 1,4,5-IP3, 1,3,4-IP3, 1,3,4,5-IP4 (Figure 1b), and STP (Figure 1d) were purchased from Wako Pure Chemical Industries, Ltd. (Osaka, Japan). D-*myo*-Phosphatidylinositol (di-C_8-PI), D-*myo*-phosphatidylinositol 4,5-bisphosphate (di-C_8-PI(4,5)P2), D-*myo*-phosphatidylinositol 3,4-bisphosphate (di-C_8-PI(3,4)P2), and D-*myo*-phosphatidylinositol 3,4,5-trisphosphate (di-C_8-PI(3,4,5)P3) (Figure 1c) were purchased from Echelon Biosciences Inc. (Salt Lake City, UT).

Plasmids, Cells, and Transfection. The vector pSG-Gag (p24) cFLAG (*22*) was used to express the $Pr55^{Gag}$ CA domain. Expression vectors for $Pr55^{Gag}$ and the MA domain, designated as pSG-Gag cFLAG and pSG-Gag (p17) cFLAG, respectively, were constructed by replacement of the *gag*-p24 gene of pSG-Gag (p24) cFLAG with PCR-amplified *gag*-related gene sequences containing *Eco*RI and *Xho*I sites at the 5′ and 3′ ends, respectively. Plasmid pNL4-3 (*23*) was used as a template for PCR. Other expression vectors for $Pr55^{Gag}$, MA, and CA (designated pEF-Gag cFLAG, pEF-Gag (p17) cFLAG, and pEF-Gag (p24) cFLAG, respectively) were constructed by inserting the *Eco*RI−*Xba*I fragment of pSG-Gag cFLAG, pSG-Gag (p17) cFLAG, and pSG-Gag (p24) cFLAG into the *Eco*RI and *Xba*I sites of pEF1/Myc-HisA (Invitrogen Corp., Carlsbad, CA), respectively. 293T cells (*24*) were cultured in Dulbecco's modified Eagle medium supplemented with 10% heat-inactivated FBS. The calcium phosphate coprecipitation method (*23*) was used for the transfection of 293T cells. Transfected cells were cultured at 37 °C for 48 h before use in western immunoblotting or protein purification.

Western Immunoblotting. Western immunoblotting was performed essentially as described elsewhere (*25*). Cell lysates

of vector-transfected 293T cells were prepared using Laemmli's (*26*) sample buffer and resolved by sodium dodecyl sulfate−polyacrylamide gel electrophoresis (SDS−PAGE). Resolved proteins were electrophoretically transferred to polyvinylidene fluoride membranes, and the membranes were treated with anti-FLAG M2 monoclonal antibody (Ab) (Sigma-Aldrich, St. Louis, MO). For visualization, ECL Plus western blotting detection reagents (Amersham Biosciences, Buckinghamshire, U.K.) were used.

Protein Purification. Vector-transfected 293T cells were lysed with TNE buffer (10 mM Tris-HCl, 150 mM NaCl, 1 mM EDTA, 1% NP-40, and 10 μg/mL aprotinin, pH 7.8) containing 1 mM dithiothreitol (DTT). After centrifugation (12000 rpm, 4 °C, 5 min), the supernatant was mixed with Sepharose CL-4B (Sigma-Aldrich, St. Louis, MO), and the resulting suspension was incubated for 2 h at 4 °C. This incubation was repeated twice, and the final supernatant was treated with mouse anti-FLAG M2 affinity gel (Sigma-Aldrich, St. Louis, MO) and 0.5 ng/mL 1× FLAG peptide (Sigma-Aldrich, St. Louis, MO), to remove nonspecific components interacting with the FLAG antibody, and incubated for 8 h at 4 °C. The beads were washed five times with TNE buffer plus 1 mM DTT. A solution of 150 μg/mL 3× FLAG peptide (Sigma-Aldrich, St. Louis, MO) in TBS buffer (50 mM Tris-HCl and 150 mM NaCl, pH 7.4) with 1 mM DTT was loaded onto the beads and incubated for 30 min at 4 °C. Following centrifugation, the resulting supernatant was used for the SPR assay.

Protein Quantification. The cFLAG proteins were resolved by SDS−PAGE followed by Coomassie Brilliant Blue (CBB) staining. Each gel band was quantified using ImageJ (version 1.38x) software, and protein concentrations were determined by comparing the intensity of protein bands with the intensity of a protein marker.

SPR Studies. A BIACORE2000 (GE Healthcare, BIACORE AB, Uppsala, Sweden) was used as the surface plasmon resonance biosensor. To prepare the IP4 immobilized sensor chip surface for the BIACORE, biotinylated IP4 in HEPES buffer (50 mM HEPES, 500 mM NaCl, 3.4 mM EDTA, and 0.005% Tween 20, pH 7.4) was injected over streptavidin covalently immobilized upon the sensor chip surface (Sensor Chip SA, GE Healthcare, BIACORE AB, Uppsala, Sweden) until a suitable level was achieved. The flow buffer contained 10 mM HEPES, 150 mM NaCl, 3.4 mM EDTA, 0.005% Tween 20, 2% (v/v) glycerol, and 0.5 mg/mL BSA (pH 7.8). Purified proteins were dialyzed against flow buffer and injected over the immobilized IP4 sensor chip. Association was followed for 3 min, and dissociation was measured at a flow rate of 20 μL/min at 25 °C. The surfaces were regenerated by injecting three 15 s pulses of 50 mM NaOH in 1 M NaCl, three 15 s pulses of 50 mM NaOH, and then a single 15 s pulse of 10 μM 1,3,4,5-IP4. The resulting surfaces were postconditioned by injecting three 15 s pulses of 10 mM NaOH. Analysis of the response was performed using evaluation software supplied with the instrument (BIAevaluation version 3.1). To eliminate small bulk refractive change differences at the beginning and end of each injection, binding responses were referenced by subtracting the response generated across a surface modified with biotin.

Equilibrium-Binding Measurement. To determine K_D values, $Pr55^{Gag}$ and MA at concentrations of 0.08 and 2.0 μM, respectively, were mixed with various concentrations of inositol phosphate, various phosphatidylinositols, or STP (only for $Pr55^{Gag}$). After reaching equilibrium (less than 30 min in all cases at 25 °C), 60 μL of each mixture was injected over the IP4 surface at 20 μL/min to quantify the free $Pr55^{Gag}$ or MA remaining in the equilibrium mixture. The K_D was obtained by fitting the data to a solution affinity model using BIAevaluation 3.1: $A_{free} = 0.5(B - A - K_D) + (0.25(A + B + K_D)^2 - AB)^{0.5}$, where A = initial concentration of proteins, A_{free} = concentration of unbound proteins remaining in the equilibrium mixture, and B = initial concentration of IP4.

RESULTS

Due to its high sensitivity, the SPR sensor (*27*, *28*) was considered the most suitable method for evaluating the weak binding affinity between Gag proteins and phosphoinositide derivatives. Two configurations were possible for SPR analysis: a system employing phosphoinositide derivatives as the ligand fixed on the sensor chip and protein analytes flowing over the ligand, or vice versa. The former system was considered the most sensitive, since the higher the molecular weight of the analyte, the larger the response unit (RU) value. Thus, we used phosphoinositides as the ligand and proteins as the analyte. Biotinylated IP4 (Figure 1a), carrying biotin through a C_6 linker (*21*), was immobilized to the streptavidin sensor chip in the SPR system through the biotin−avidin interaction.[2] As only a small amount of protein is sufficient for this system, we employed mammalian cells rather than *Escherichia coli* to produce proteins with a more native character. That the MA thus produced was myristoylated was confirmed by MALDI-TOF-MS; no contamination by unmyristoylated MA was detected (Figure 6, Supporting Information).

Expression vectors for full-length $Pr55^{Gag}$, MA, and CA containing a FLAG tag at the C-terminus were prepared. Plasmid vectors with different promoters were constructed based on pSG5 and pEF1/Myc-HisA, and protein expression in 293T cells transfected with these vectors was evaluated by western immunoblotting using anti-FLAG Ab (data not shown). Vectors from pEF1/Myc-HisA expressed larger amounts of MA and CA protein compared with vectors from pSG5 (MA, about 10-fold increase; CA, about 2-fold increase). On the other hand, the expression of $Pr55^{Gag}$ from the vector based on pEF/Myc-HisA was markedly lower compared to expression based on pSG5. Thus, pEF/Myc-HisA-based vectors were used for the expression of MA and CA, and the pSG5-based vector was used for $Pr55^{Gag}$ expression. Proteins were purified from transfected 293T cells using anti-FLAG agarose beads employing the FLAG tag affinity method. Purified proteins were quantified by SDS−PAGE analysis (Figure 2), and their concentration was estimated by comparing the band intensity with that of the protein marker: the concentrations of MA, CA, and $Pr55^{Gag}$ were 2.0, 5.5, and 0.08 μM, respectively.

After purification, the solution in which each protein dissolved was exchanged with flow buffer in the SPR system through dialysis. Flow buffer was supplemented with 0.5 mg/mL BSA to inhibit nonselective binding to the biotin-modified control surface, followed by 2% (v/v) glycerol to prevent protein destabilization (*29*). Association was followed for 3 min, and dissociation was measured at a flow rate of 20 μL/min at 25 °C, after which the surfaces were regenerated by injecting dilute NaOH solution. As shown in Figure 3, the injection of either

[2]IP4 was preferred to other phosphoinositides for immobilization owing to the fidelity of the data. Immobilization of tethered di-C_8-PI(4,5)P2 accompanied nonspecific binding, and sometimes partial hydrolysis of acyl groups took place, depending on the solution conditions (data not shown); therefore, we employed biotinylated IP4.

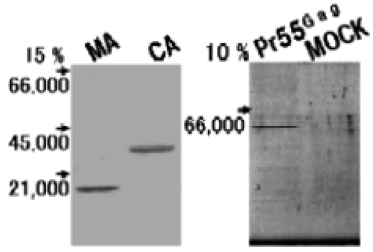

FIGURE 2: SDS−PAGE analysis of Gag-related proteins. After purification, protein solutions were resolved on 10% and 15% SDS−PAGE gels and visualized by CBB staining. Protein concentrations estimated by comparison to molecular weight marker intensity were MA = 2.0 μM, CA = 5.5 μM, and $Pr55^{Gag}$ = 0.08 μM.

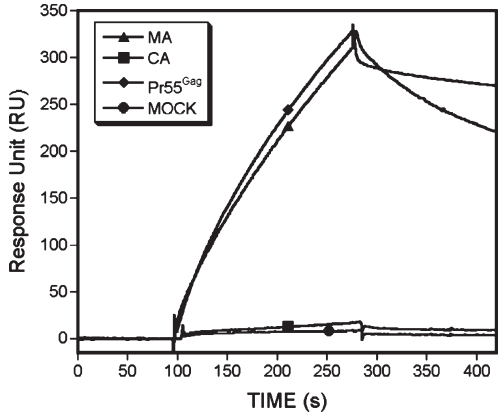

FIGURE 3: Binding activity of Gag-related proteins to biotinylated IP4. Each protein was injected over a biotinylated IP4 immobilized sensor chip at flow rate of 20 μL/min for 180 s.

$Pr55^{Gag}$ (0.08 μM) or MA (2.0 μM) onto immobilized IP4 induced a rising slope up to approximately 300 RU, indicating that $Pr55^{Gag}$ and MA interact with IP4. Affinity for IP4 was not observed with injection of CA.

The K_D of $Pr55^{Gag}$/MA−phosphoinositide complexes were calculated using a competition assay. The competitors used in this study are shown in Figure 1b−d. Second messengers 1,4,5-IP3, 1,3,4-IP3 (a regioisomer of 1,4,5-IP3), and 3-phospho 1,3,4,5-IP4 served as inositol phosphate derivatives. To confirm the significance of the charge interaction in the inositol skeleton, competition with STP was examined. Di-C_8-PI (which has a lipid moiety attached through a phosphodiester linkage and is devoid of the other phosphate groups), as well as di-C_8-PI(4,5)P2, di-C_8-PI(3,4)P2, and di-C_8-PI(3,4,5)P3 (which have both lipid and divalent phosphate groups), were used as competitors.

Varying concentrations of each competitor were preincubated with $Pr55^{Gag}$ and passed over the immobilized IP4 surface. The RU curves for competition between $Pr55^{Gag}$ and the various competitors are shown in Figure 4a,c,e,g,i,k,m,o; the corresponding K_D values are shown in Figure 4b,d,f,h,j,l,n,p. As shown in Figure 4a, 1,4,5-IP3 competed with immobilized IP4 in a concentration-dependent manner to displace $Pr55^{Gag}$ from IP4, causing a decrease in RU. However, complete competitive displacement did not occur even at a 1,4,5-IP3 concentration of 5 mM. As PI does not dissolve in buffer, soluble di-C_8-PI possessing saturated shorter C_6 acyl chains was utilized for this study, resulting in more effective competition (Figure 4i). As shown in Figure 4k, di-C_8-PI(4,5)P2 competed with even greater efficiency, as almost complete displacement of $Pr55^{Gag}$ was observed at a di-C_8-PI(4,5)P2 concentration of 250 μM.

The competition curves were obtained by setting the concentration of competitors upon the horizontal axis and the response of free $Pr55^{Gag}$, determined based on the concentration of $Pr55^{Gag}$ bound to IP4, upon the vertical axis. The K_D values for $Pr55^{Gag}$ in competition with 1,4,5-IP3, di-C_8-PI, and di-C_8-PI(4,5)P2 were 2170 (Figure 4b), 186 (Figure 4j), and 47.4 μM (Figure 4l), respectively. The dissociation constant for di-C_8-PI(4,5)P2 was 46 times lower than the K_D for 1,4,5-IP3 and 4 times lower than the K_D for di-C_8-PI.

The K_D values of $Pr55^{Gag}$ complexed with the other competitors are shown in Table 1. The binding affinity between 1,3,4-IP3 and $Pr55^{Gag}$ (K_D = 579 μM) (Figure 4d) was 4 times greater than that of 1,4,5-IP3 (K_D = 2170 μM). The affinity of 1,3,4,5-IP4 (K_D = 332 μM) (Figure 4f) was 2 times greater than that of 1,3,4-IP3. STP, a tandem array of three phosphoric acids, bound $Pr55^{Gag}$ (K_D = 1810 μM) (Figure 4h) as weakly as 1,4,5-IP3 (K_D = 2170 μM). The affinity of di-C_8-PI(3,4)P2 for $Pr55^{Gag}$ (K_D = 54.6 μM) (Figure 4n) was almost the same as that of di-C_8-PI(4,5)P2 (K_D = 47.4 μM), while the binding affinity of di-C_8-PI(3,4,5)P3 (K_D = 19.3 μM) (Figure 4p) was 2 times greater than that of di-C_8-PI(4,5)P2. In the case of the 1,3,4 and 1,3,4,5 derivatives, the order of K_D values (1,3,4-IP3 > di-C_8-PI > di-C_8-PI(3,4)P2, 1,3,4,5-IP4 > di-C_8-PI > di-C_8-PI(3,4,5)P3) was the same as that observed for the 1,4,5 derivatives.

We also examined the affinity between MA and various phosphoinositides, as shown in Table 1. The binding affinities of 1,4,5-IP3 (K_D = 568 μM) (Figure 5b) and 1,3,4,5-IP4 (K_D = 526 μM) (Figure 5d) for MA were almost identical. The K_D of di-C_8-PI was 178 μM (Figure 5f), while those of di-C_8-PI(4,5)P2, di-C_8-PI(3,4)P2, and di-C_8-PI(3,4,5)P3 were 5.64, 2.51, and 6.02 μM, respectively (Figure 5h,j,l). The order of K_D values for binding between MA and various competitors (1,4,5-IP3 > di-C_8-PI > di-C_8-PI(4,5)P2, 1,3,4,5-IP4 > di-C_8-PI > di-C_8-PI-(3,4,5)P3) was the same as that found for binding to $Pr55^{Gag}$. The affinity of the shorter acyl chain competitor di-C_4-PI(4,5)P2 for MA (K_D = 86.6 μM) (Figure 5n) was 15 times weaker than the affinity between di-C_8-PI(4,5)P2 and MA.

DISCUSSION

In this study, we developed a new SPR sensor-based technique to observe the binding affinity between proteins and phosphoinositide derivatives. This assay system is convenient and highly sensitive, enabling detection of weak binding (K_D > 2000 μM). Using this method, we determined the K_D for interaction between $Pr55^{Gag}$ or MA and various phosphoinositide derivatives and related compounds. The MA used in this study was produced by mammalian cells and was shown by MS analysis to be myristoylated (Figure 6, Supporting Information).

Other researchers have suggested that $Pr55^{Gag}$ directly interacts with PI(4,5)P2 (*11*−*13*). However, the roles played by the acyl group and the negatively charged inositol headgroups in the binding of PI(4,5)P2 to $Pr55^{Gag}$ have not been fully elucidated. To more fully define these interactions, we examined the binding affinity between $Pr55^{Gag}$ and 1,4,5-IP3, which has divalent phosphate groups at the 1,4,5-position of the inositol headgroup and lacks an acyl tail. We found that 1,4,5-IP3 binds $Pr55^{Gag}$ very weakly (K_D = 2170 μM). We then determined the binding affinity between $Pr55^{Gag}$ and di-C_8-PI, which is composed of a glycerol tail containing saturated C_6 acyl chains and inositol devoid of divalent phosphate groups. Unexpectedly, di-C_8-PI bound $Pr55^{Gag}$ with an affinity 12 times greater (K_D = 186 μM) than

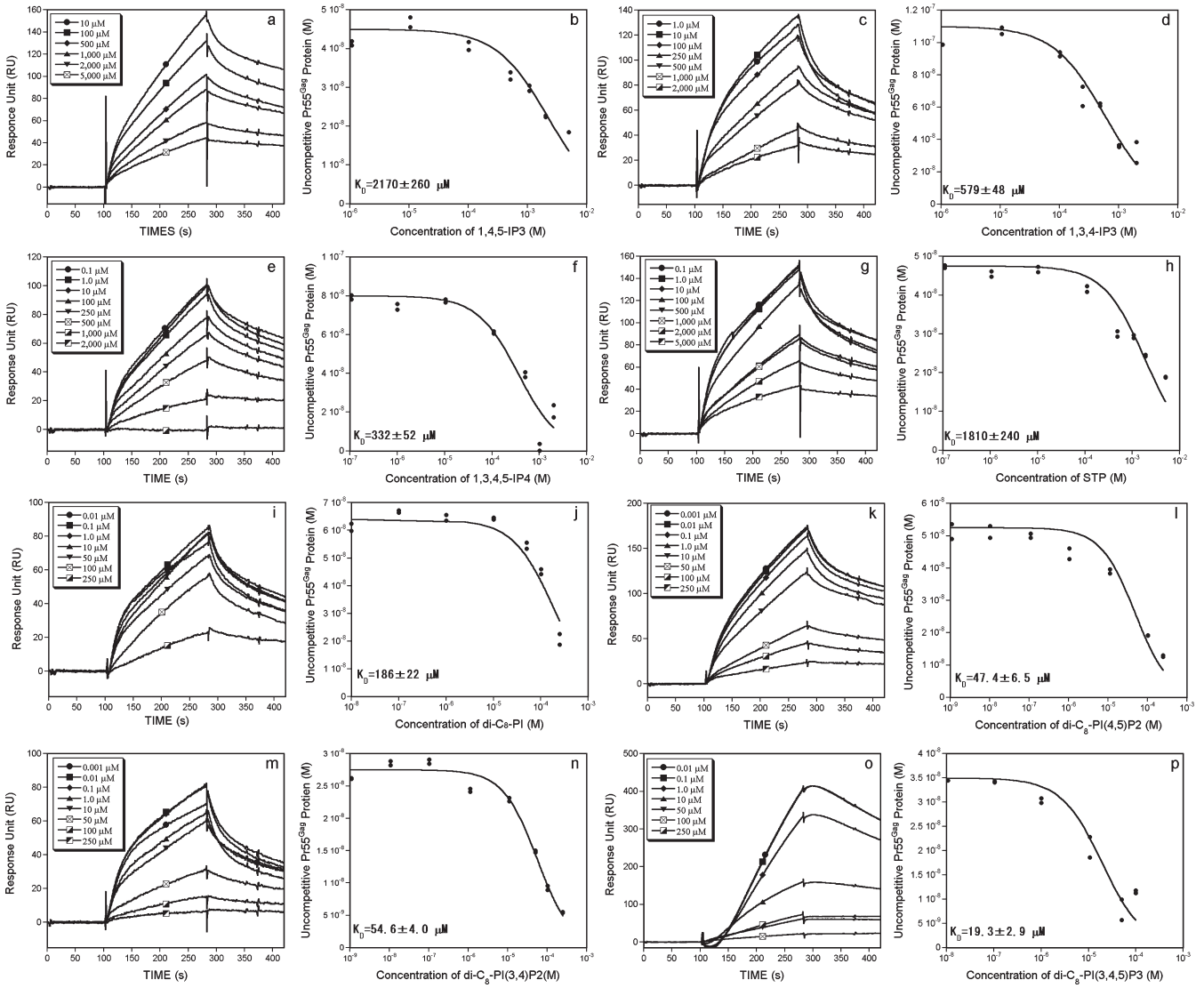

FIGURE 4: Competition assay and calculation of the equilibrium dissociation constants (K_D) for $Pr55^{Gag}$−competitor complexes. The equilibrium mixtures of $Pr55^{Gag}$ and competitors 1,4,5-IP3 (a), 1,3,4-IP3 (c), 1,3,4,5-IP4 (e), STP (g), di-C_8-PI (i), di-C_8-PI(4,5)P2 (k), di-C_8-PI(3,4)P2 (m), and di-C_8-PI(4,5)P2 (o) were injected over the biotinylated IP4 immobilized sensor chip at a flow rate of 20 μL/min for 180 s. The average response unit (RU) for the increasing concentration of each competitor was measured at 160−170 s, and each RU datum was converted to a concentration of uncompetitive $Pr55^{Gag}$ protein used for the construction of competition curves between uncompetitive $Pr55^{Gag}$ and 1,4,5-IP3 (b), 1,3,4-IP3 (d), 1,3,4,5-IP4 (f), STP (h), di-C_8-PI (j), di-C_8-PI(4,5)P2 (l), di-C_8-PI(3,4)P2 (n), and di-C_8-PI(4,5)P2 (p). Calculated K_D values are shown. Each experiment was performed in duplicate.

that of 1,4,5-IP3 (K_D = 2170 μM). The K_D for the interaction of $Pr55^{Gag}$ and di-C_8-PI(4,5)P2, which has divalent phosphate groups at the 4,5-position of the inositol headgroup and saturated C_6 acyl chains, was 47.4 μM. McLaughlin and Aderem suggested that the myristoyl group of $Pr55^{Gag}$ binds to lipid bilayers with a K_D of approximately 100 μM (*30*); thus, the binding affinity we determined for di-C_8-PI(4,5)P2 (K_D = 47.4 μM) is sufficient for membrane binding of $Pr55^{Gag}$. In addition, the binding affinity of di-C_8-PI(4,5)P2 was 46 and 4 times greater than that of 1,4,5-IP3 and di-C_8-PI, respectively. The same tendency was observed in the case of complexes of other phosphoinositide derivatives and MA. These data suggest that both phosphate groups and acyl chains are essential for tight binding between $Pr55^{Gag}$ and phosphoinositides and that the presence of the acyl chains is more important than the inositol divalent phosphate groups.

The mode whereby $Pr55^{Gag}$ binds to form a complex with PI(4,5)P2 was determined by NMR studies (*12*). The hydrophobic region of $Pr55^{Gag}$ attracts the PI(4,5)P2 2′-acyl chain, while the $Pr55^{Gag}$ myristoyl group adopts exposed conformations. The positively charged region of $Pr55^{Gag}$ accommodates the negatively charged inositol headgroup neighboring the 2′-acyl chain site. Eventually, these interactions would work to stabilize the $Pr55^{Gag}$−PI(4,5)P2 complex. Thus, the inositol moiety and lipid group are believed to bind $Pr55^{Gag}$ through electrostatic interaction and hydrophobic interaction, respectively. Considering the stronger binding affinity of the $Pr55^{Gag}$−di-C_8-PI complex (K_D = 186 μM) compared to the $Pr55^{Gag}$−1,4,5-IP3 complex (K_D = 2170 μM), we suggest that hydrophobic interaction contributes more markedly than electrostatic interactions. Alfadhli et al. demonstrated the significance of the myristoyl group by comparing the effect of di-C_8-PI(4,5)P2 on liposome binding of myristoylated and nonmyristoylated MA. Their work suggested that di-C_8-PI(4,5)P2 can trigger myristate exposure (*31*).

We observed that 1,4,5-IP3 and STP bound $Pr55^{Gag}$ with essentially the same (albeit weak) affinity (K_D = 2170 and 1810 μM,

Table 1: K_D Values for $Pr55^{Gag}$ or MA Complexed with Phosphoinositide-Related Compounds

proteins	competitors	K_D (μM)
$Pr55^{Gag}$	inositol phosphates	
	1,4,5-IP3	2170 ± 260
	1,3,4-IP3	579 ± 48
	1,3,4,5-IP4	332 ± 58
	phosphate	
	STP	1810 ± 240
	phosphatidylinositols	
	di-C_8-PI	186 ± 22
	di-C_8-PI(4,5)P2	47.4 ± 6.5
	di-C_8-PI(3,4)P2	54.6 ± 4.8
	di-C_8-PI(3,4,5)P3	19.3 ± 2.9
MA	inositol phosphates	
	1,4,5-IP3	568 ± 52
	1,3,4,5-IP4	526 ± 57
	phosphatidylinositols	
	di-C_8-PI	178 ± 29
	di-C_8-PI(4,5)P2	5.64 ± 1.43
	di-C_8-PI(3,4)P2	2.51 ± 1.56
	di-C_8-PI(3,4,5)P3	6.02 ± 0.97
	di-C_4-PI(4,5)P2	86.6 ± 2.2

respectively), suggesting that the specific configuration of phosphate groups is not the only factor influencing binding of $Pr55^{Gag}$ and 1,4,5-IP3. On the other hand, the $Pr55^{Gag}$-binding affinities of 1,3,4-IP3 and 1,3,4,5-IP4 (K_D = 579 and 332 μM, respectively) were greater than that of 1,4,5-IP3, suggesting that the 3-phosphate group plays a significant role in binding in this case. The K_D we determined for the $Pr55^{Gag}$−1,3,4,5-IP4 complex (332 μM) could be accounted for by the presence of the 3-phosphate group in addition to the other three phosphate groups. In contrast to the inositol phosphates, di-C_8-PI(4,5)P2 and di-C_8-PI(3,4)P2 had essentially the same affinity for $Pr55^{Gag}$ (K_D = 47.4 and 54.6 μM, respectively), suggesting that differences in the electrostatic interaction of the phosphates were negated by the hydrophobic interaction of the acyl chains. The binding of di-C_8-PI(3,4,5)P3 to $Pr55^{Gag}$ (K_D = 19.3 μM) was markedly stronger than that of di-C_8-PI(3,4)P2 (K_D = 54.6 μM) and di-C_8-PI(4,5)P2 (K_D = 47.4 μM). Chukkapalli et al. (*32*) reported that $Pr55^{Gag}$ binds to liposomes containing either PI(4,5)P2 or PI(3,4,5)P3 with essentially the same affinity. As PI(4,5)P2 and PI(3,4,5)P3 contain C_{17}/C_{19} lipid groups, the apparent discrepancy in $Pr55^{Gag}$ binding affinity between PI and di-C_8-PI may be due to difference in the chain length.

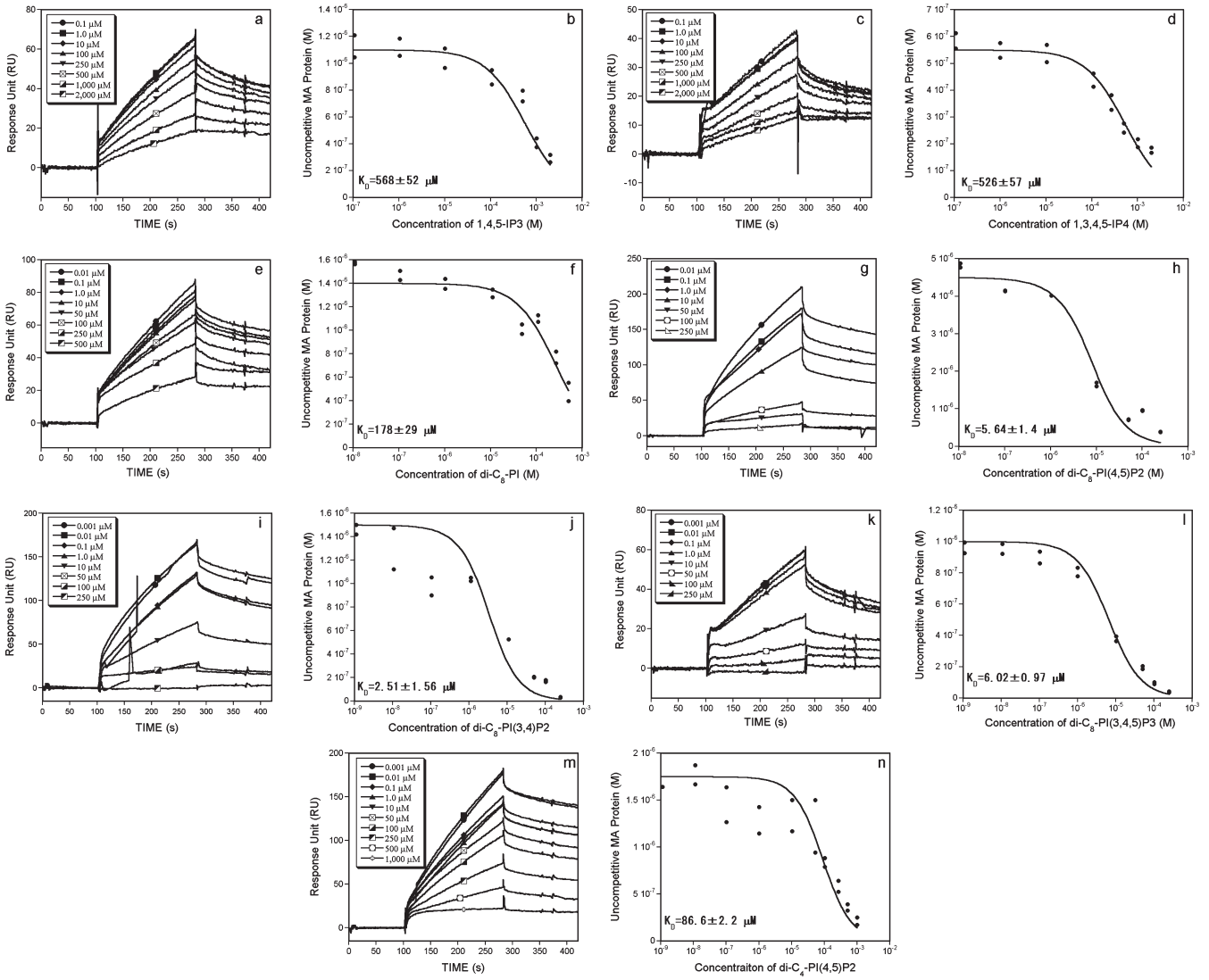

FIGURE 5: Competitive assay and calculation of the equilibrium dissociation constants (K_D) for MA−competitor complexes. The arrangement is the same as that in Figure 4 (a and b, 1,4,5-IP3; c and d, 1,3,4,5-IP4; e and f, di-C_8-PI; g and h, di-C_8-PI(4,5)P2; i and j, di-C_8-PI(3,4)P2; k and l, di-C_8-PI(3,4,5)P3; m and n, di-C_4-PI(4,5)P2).

The binding affinity between phosphoinositides and the MA domain was more consistent than was the case with $Pr55^{Gag}$, as we found that K_D values for MA-di-C_8-PI(4,5)P2, MA-di-C_8-PI(3,4)P2, and MA-di-C_8-PI(3,4,5)P3 complexes were almost the same (5.64, 2.51, and 6.02 μM, respectively). Using NMR, Saad et al. (*12*) reported K_D values for di-C_4-PI(4,5)P2 and di-C_4-PI(3,4,5)P3 (both of which have C_2 acyl chains) binding to MA of 150 and 81 μM, respectively. Using our surface plasmon resonance approach, we determined a K_D value of 86.6 μM (Figure 5n) for the MA−di-C_4-PI(4,5)P2 complex, a value that is consistent with the result of 150 μM reported by Saad et al. The deviation between the observations could be due to the experimental methods, i.e., SPR and NMR. These data suggest that a longer carbon chain contributes to the enhancement of MA affinity. Despite the slight difference in K_D, both NMR and our SPR findings suggest that in the viral replication cycle MA can still interact with phosphoinositides after the cleavage of $Pr55^{Gag}$. Furthermore, the binding affinity between MA and 1,3,4,5-IP4 (K_D = 526 μM), in which there is a greater degree of electrostatic charge, was virtually identical to the affinity between MA and 1,4,5-IP3 (K_D = 568 μM). A previous study revealed that the mature MA domain might be folded differently than it is in the full-length $Pr55^{Gag}$ protein (*33*). This could account for the similar K_D values (526 and 568 μM, respectively) observed for the binding of MA to 1,3,4,5-IP4 and 1,4,5-IP3.

Saad et al. (*12*) reported that di-C_8 acyl chain competitor molecules induced the aggregation of MA, and as a result, they were unable to determine the K_D. Fortunately, we did not observe any apparent aggregation or precipitation in our experiments, however. Competition curves indicated that both di-C_4-PI(4,5)P2 and di-C_8-PI(4,5)P2 interacted in a concentration-dependent manner. This could be due to the conditions used in our experiments. The flow buffer used in our assay was supplemented with 0.5 mg/mL BSA and 2% (v/v) glycerol to stabilize protein structure and 0.005% Tween 20 as a detergent; thus it is thought that the amount of the aggregation is negligible.

It is possible that the acyl chains of di-C_8-PIPs may interact hydrophobically with myristate rather than with the MA hydrophobic cleft in our SPR assay using myristoylated MA. However, as demonstrated by Alphadhali et al. (*31*), di-C_4-PI(4,5)P2 and di-C_8-PI(4,5)P2 can trigger myristate exposure in MA. This is especially true for di-C_8-PI(4,5)P2, which has longer acyl chains. Furthermore, in the NMR assay employed by Saad et al. (*12*), the hydrophobic region of MA attracts only the 2′-acyl chain of di-C_4-PI(4,5)P2 as a result of the nuclear Overhauser effect. In our SPR assay, the 2′-acyl chain is presumed to interact hydrophobically with the hydrophobic cleft, exposing the MA myristate moiety.

The pleckstrin homology (PH) domain is a well-known phosphoinositide-binding motif (*34*−*36*) found in more than 100 proteins. The phospholipase C (PLC) δ_1 PH domain interacts with 1,4,5-IP3 and 1,3,4,5-IP4 with a K_D of 0.21 and 13.4 μM, respectively (*36*, *37*). The structural basis for the specificity in PH-1,4,5-IP3 binding is attributed to direct hydrogen bonding between 1,4,5-IP3 and several amino acid residues (*38*). Interactions between PH and phosphoinositides are predominated by electrostatic interactions, unlike binding between phosphoinositides and $Pr55^{Gag}$, where hydrophobic interactions of the acyl chains lower binding affinity.

We observed relatively strong affinity with only slight differences in K_D between $Pr55^{Gag}$ and di-C_8-PI(4,5)P2 (47.4 μM) and di-C_8-PI(3,4,5)P3 (19.3 μM). These results are most likely due to both the strong hydrophobic interaction between the hydrophobic region of $Pr55^{Gag}$ and the acyl chains of the phosphoinositides and weak hydrophilic interactions. Saad et al. (*12*) suggested that the 1,4,5-IP3 group interacts electrostatically with basic amino acids in MA during formation of the MA−di-C_4-PI(4,5)P2 complex (the 4,5-phosphate is positioned to form salt bridges with R22 and R76; the 1-phosphate is positioned so as to favorably interact electrostatically with K27 and H33). This interaction is responsible for the weaker electrostatic binding between $Pr55^{Gag}$ and phosphoinositide.

In conclusion, our results may provide a structural basis for the molecular design of novel anti-HIV agents comprising inositol phosphate and hydrophobic groups.

ACKNOWLEDGMENT

We thank Dr. Yoshihiro Yamaguchi of the Environmental Safety Center, Kumamoto University, for technical advice on protein purification.

SUPPORTING INFORMATION AVAILABLE

MALDI-TOF-MS spectrometry data of myristoylated MA. This material is available free of charge via the Internet at http://pubs.acs.org.

REFERENCES

1. Wills, J. W., and Craven, R. C. (1991) Form, function, and use of retroviral gag proteins. *AIDS 5*, 639–654.
2. Freed, E. O. (1998) HIV-1 gag proteins: diverse functions in the virus life cycle. *Virology 251*, 1–15.
3. Conte, M. R., and Matthews, S. (1998) Retroviral matrix proteins: a structural perspective. *Virology 246*, 191–198.
4. Gamble, T. R., Yoo, S., Vajdos, F. F., von Schwedler, U. K., Worthylake, D. K., Wang, H., McCutcheon, J. P., Sundquist, W. I., and Hill, C. P. (1997) Structure of the carboxyl-terminal dimerization domain of the HIV-1 capsid protein. *Science 278*, 849–853.
5. Dawson, L., and Yu, X. F. (1998) The role of nucleocapsid of HIV-1 in virus assembly. *Virology 251*, 141–157.
6. Parent, L. J., Bennett, R. P., Craven, R. C., Nelle, T. D., Krishna, N. K., Bowzard, J. B., Wilson, C. B., Puffer, B. A., Montelaro, R. C., and Wills, J. W. (1995) Positionally independent and exchangeable late budding functions of the Rous sarcoma virus and human immunodeficiency virus Gag proteins. *J. Virol. 69*, 5455–5460.
7. Nguyen, D. H., and Hildreth, J. E. (2000) Evidence for budding of human immunodeficiency virus type 1 selectively from glycolipid-enriched membrane lipid rafts. *J. Virol. 74*, 3264–3272.
8. Resh, M. D. (2004) A myristoyl switch regulates membrane binding of HIV-1 Gag. *Proc. Natl. Acad. Sci. U.S.A. 101*, 417–418.
9. Tang, C., Loeliger, E., Luncsford, P., Kinde, I., Beckett, D., and Summers, M. F. (2004) Entropic switch regulates myristate exposure in the HIV-1 matrix protein. *Proc. Natl. Acad. Sci. U.S.A. 101*, 517–522.
10. Zhou, W., Parent, L. J., Wills, J. W., and Resh, M. D. (1994) Identification of a membrane-binding domain within the amino-terminal region of human immunodeficiency virus type 1 Gag protein which interacts with acidic phospholipids. *J. Virol. 68*, 2556–2569.
11. Ono, A., Ablan, S. D., Lockett, S. J., Nagashima, K., and Freed, E. O. (2004) Phosphatidylinositol (4,5) bisphosphate regulates HIV-1 Gag targeting to the plasma membrane. *Proc. Natl. Acad. Sci. U.S.A. 101*, 14889–14894.
12. Saad, J. S., Miller, J., Tai, J., Kim, A., Ghanam, R. H., and Summers, M. F. (2006) Structural basis for targeting HIV-1 Gag proteins to the plasma membrane for virus assembly. *Proc. Natl. Acad. Sci. U.S.A. 103*, 11364–11369.
13. Shkriabai, N., Datta, S. A., Zhao, Z., Hess, S., Rein, A., and Kvaratskhelia, M. (2006) Interactions of HIV-1 Gag with assembly cofactors. *Biochemistry 45*, 4077–4083.
14. Berridge, M. J. (1993) Inositol trisphosphate and calcium signalling. *Nature 361*, 315–325.
15. Toker, A., and Cantley, L. C. (1997) Signalling through the lipid products of phosphoinositide-3-OH kinase. *Nature 387*, 673–676.
16. Steinberg, S. F. (2008) Structural basis of protein kinase C isoform function. *Physiol. Rev. 88*, 1341–1378.

17. Griner, E. M., and Kazanietz, M. G. (2007) Protein kinase C and other diacylglycerol effectors in cancer. *Nat. Rev. Cancer 7*, 281–294.
18. Caroni, P. (2001) New EMBO members' review: actin cytoskeleton regulation through modulation of PI(4,5)P(2) rafts. *EMBO J. 20*, 4332–4336.
19. Lockyer, P. J., Bottomley, J. R., Reynolds, J. S., McNulty, T. J., Venkateswarlu, K., Potter, B. V., Dempsey, C. E., and Cullen, P. J. (1997) Distinct subcellular localisations of the putative inositol 1,3,4,5-tetrakisphosphate receptors GAP1IP4BP and GAP1m result from the GAP1IP4BP PH domain directing plasma membrane targeting. *Curr. Biol. 7*, 1007–1010.
20. Divecha, N., and Irvine, R. F. (1995) Phospholipid signaling. *Cell 80*, 269–278.
21. Anraku, K., Inoue, T., Sugimoto, K., Morii, T., Mori, Y., Okamoto, Y., and Otsuka, M. (2008) Design and synthesis of biotinylated inositol phosphates relevant to the biotin-avidin techniques. *Org. Biomol. Chem. 6*, 1822–1830.
22. Fujita, M., Akari, H., Sakurai, A., Yoshida, A., Chiba, T., Tanaka, K., Strebel, K., and Adachi, A. (2004) Expression of HIV-1 accessory protein Vif is controlled uniquely to be low and optimal by proteasome degradation. *Microbes Infect. 6*, 791–798.
23. Adachi, A., Gendelman, H. E., Koenig, S., Folks, T., Willey, R., Rabson, A., and Martin, M. A. (1986) Production of acquired immunodeficiency syndrome-associated retrovirus in human and nonhuman cells transfected with an infectious molecular clone. *J. Virol. 59*, 284–291.
24. Lebkowski, J. S., Clancy, S., and Calos, M. P. (1985) Simian virus 40 replication in adenovirus-transformed human cells antagonizes gene expression. *Nature 317*, 169–171.
25. Willey, R. L., Smith, D. H., Lasky, L. A., Theodore, T. S., Earl, P. L., Moss, B., Capon, D. J., and Martin, M. A. (1988) In vitro mutagenesis identifies a region within the envelope gene of the human immunodeficiency virus that is critical for infectivity. *J. Virol. 62*, 139–147.
26. Laemmli, U. K. (1970) Cleavage of structural proteins during the assembly of the head of bacteriophage T4. *Nature 227*, 680–685.
27. Johnsson, B., Lofas, S., and Lindquist, G. (1991) Immobilization of proteins to a carboxymethyldextran-modified gold surface for biospecific interaction analysis in surface plasmon resonance sensors. *Anal. Biochem. 198*, 268–277.
28. Karlsson, R. (1994) Real-time competitive kinetic analysis of interactions between low-molecular-weight ligands in solution and surface-immobilized receptors. *Anal. Biochem. 221*, 142–151.
29. Ferguson, C. G., James, R. D., Bigman, C. S., Shepard, D. A., Abdiche, Y., Katsamba, P. S., Myszka, D. G., and Prestwich, G. D. (2005) Phosphoinositide-containing polymerized liposomes: stable membrane-mimetic vesicles for protein-lipid binding analysis. *Bioconjugate Chem. 16*, 1475–1483.
30. McLaughlin, S., and Aderem, A. (1995) The myristoyl-electrostatic switch: a modulator of reversible protein-membrane interactions. *Trends Biochem. Sci. 20*, 272–276.
31. Alfadhli, A., Still, A., and Barklis, E. (2009) Analysis of human immunodeficiency virus type 1 matrix binding to membranes and nucleic acids. *J. Virol. 83*, 12196–12203.
32. Chukkapalli, V., Hogue, I. B., Boyko, V., Hu, W. S., and Ono, A. (2008) Interaction between the human immunodeficiency virus type 1 Gag matrix domain and phosphatidylinositol-(4,5)-bisphosphate is essential for efficient gag membrane binding. *J. Virol. 82*, 2405–2417.
33. Datta, S. A., Curtis, J. E., Ratcliff, W., Clark, P. K., Crist, R. M., Lebowitz, J., Krueger, S., and Rein, A. (2007) Conformation of the HIV-1 Gag protein in solution. *J. Mol. Biol. 365*, 812–824.
34. Harlan, J. E., Hajduk, P. J., Yoon, H. S., and Fesik, S. W. (1994) Pleckstrin homology domains bind to phosphatidylinositol-4,5-bisphosphate. *Nature 371*, 168–170.
35. Hyvonen, M., Macias, M. J., Nilges, M., Oschkinat, H., Saraste, M., and Wilmanns, M. (1995) Structure of the binding site for inositol phosphates in a PH domain. *EMBO J. 14*, 4676–4685.
36. Lemmon, M. A., Ferguson, K. M., O'Brien, R., Sigler, P. B., and Schlessinger, J. (1995) Specific and high-affinity binding of inositol phosphates to an isolated pleckstrin homology domain. *Proc. Natl. Acad. Sci. U.S.A. 92*, 10472–10476.
37. Kavran, J. M., Klein, D. E., Lee, A., Falasca, M., Isakoff, S. J., Skolnik, E. Y., and Lemmon, M. A. (1998) Specificity and promiscuity in phosphoinositide binding by pleckstrin homology domains. *J. Biol. Chem. 273*, 30497–30508.
38. Ferguson, K. M., Lemmon, M. A., Schlessinger, J., and Sigler, P. B. (1995) Structure of the high affinity complex of inositol trisphosphate with a phospholipase C pleckstrin homology domain. *Cell 83*, 1037–1046.